Single-cell RNA-seq reveals profound monocyte changes in Paediatric Inflammatory Multisystem Syndrome Temporally associated with SARS-CoV-2 infection (PIMS-TS)

Eleni Syrimi[1*], Eanna Fennell[2*], Alex Richter[3], Pavle Vrljicak[4], Richard Stark[5], Sascha Ott[4,5], Paul G Murray[2], Eslam Al-Abadi[6], Ashish Chikermane[6], Pamela Dawson[6], Scott Hackett[7], Steven Welch[7], Deepthi Jyothish[6], Hari Krishnan Kanthimathinathan[6], Sean Monaghan[6], Prasad Nagakumar[6,8], Barnaby R Scholefield[6,8], Pamela Kearns[9§], Graham S Taylor[1§].

[1] Institute of Immunology and Immunotherapy, University of Birmingham, Birmingham, B15 2TT, UK.
[2] Health Research Institute and the Bernal Institute, University of Limerick, Limerick, Ireland
[3] Clinical Immunology Service, Institute of Immunology and Immunotherapy, University of Birmingham, Birmingham, B15 2TT, UK.
[4] Warwick Medical School, University of Warwick, Coventry, UK.
[5] Bioinformatics Research Technology Platform, University of Warwick, Coventry, UK.
[6] Birmingham Women's and Children's NHS Foundation Trust, Birmingham, UK.
[7] Heartlands Hospital, University Hospitals Birmingham NHS Foundation Trust, Birmingham, UK.
[8] Institute of Inflammation and Ageing, University of Birmingham, Birmingham, UK.
[9] NIHR Birmingham Biomedical Research Centre and Institute of Cancer and Genomic Sciences, University of Birmingham, Birmingham, UK.

*Equal contribution

[§]Correspondence: P.R.Kearns@bham.ac.uk; G.S.Taylor@bham.ac.uk

Abstract

Paediatric inflammatory multisystem inflammatory syndrome temporally associated with SARS-CoV-2 infection (PIMS-TS) is a new disease with overlapping features of Kawasaki disease (KD) and toxic shock syndrome. Unbiased single cell RNA sequencing analysis of peripheral blood mononuclear cells from PIMS-TS and KD patients shows monocytes are the main source of pro-inflammatory cytokines and large changes in the frequency of classical, intermediate and non-classical monocytes occur in both diseases.

MAIN

SARS-CoV-2, the viral cause of coronavirus disease 2019 (Covid-19), usually causes mild respiratory infection in children and young adults [1]. Multiple reports show some children subsequently develop a severe hyperinflammatory syndrome comprising fever, inflammation and evidence of single or multi-organ failure that manifests with cardiac dysfunction, hypotension and life-threatening shock [2,3,4]. This new disease, called Paediatric inflammatory multisystem inflammatory syndrome temporally associated with SARS-CoV-2 infection (PIMS-TS, also known as multisystem inflammatory syndrome in children MIS-C) occurs several weeks after SARS-CoV-2 infection which may or may not have been symptomatic. PIMS-TS shares clinical features with Kawasaki Disease (KD) a vasculitis affecting mostly children <5 years old that can present with features of systemic and cardiac inflammation [5,6]. KD can lead to fatal coronary artery aneurysms and is the leading cause of acquired heart disease in children in developed nations. This risk is significantly reduced with early treatment using intravenous immunoglobulin (IVIG) although 20% of patients require additional interventions due to failure to respond to initial treatment [6]. The immunology of KD is still not fully understood but patient data and animal models suggest monocytes are involved [5,7,8]. The CAWS mouse model of KD shows increased recruitment and accumulation of bone marrow derived monocytes into the heart and the inflammatory cytokine IL1-beta are both essential for pathogenesis [8]. Given the recent emergence of PIMS-TS, little is known about the immunological processes driving the disease and whether these are similar or different to KD.

We recruited nine children with signs of PIMS-TS or KD who presented at Birmingham Children's Hospital from April to May 2020. Demographic and clinical features are presented in Figure 1 and SI Table 1 and 2. Seven children met the UK's Royal College of Paediatrics and Child Health case definition of PIMS-TS and were SARS-CoV-2 antibody positive. Two children fulfilled the KD criteria [6] and were SARS-CoV-2 antibody negative. Disease severity varied markedly. Neither of the KD patients required Paediatric Intensive Care Unit (PICU) admission whereas 5/7 PIMS-TS patients required PICU for 3 to 8 days (Figure 1B). A range of treatment intensities were required to achieve clinical response. All PIMS-TS patients were lymphopaenic and four had elevated neutrophils (Figure 1C). Frequencies of T and B cells were variable but the frequency and absolute counts of NK cells were low in PIMS-TS patients compared to KD (Figure 1D).

To resolve the complexity and heterogeneity of cellular immune subsets in the blood of patients with PIMS-TS, we performed unbiased single cell RNA sequencing (scRNAseq) on the pre-treatment peripheral blood mononuclear cells (PMBCs) of two representative patients

with PIMS-TS, P6 and P7. Both were admitted to PICU but patient P7 responded rapidly to one cycle of IVIG whereas patient P6 required additional IVIG, steroids and Tocilizumab. A convalescent sample from P6 was also analysed. For comparative purposes we analysed pre-treatment PBMCs from a KD patient (KD2) who similarly required multiple treatment cycles (Figure 1B). Unsupervised clustering of 10,031 cells produced 19 different clusters comprising all major lymphocyte subsets (Figure 1E, SI Fig 1 and 2). Examining cytokine mRNA data showed monocytes were by far the predominant cell type expressing IL1-beta, TNF-a, IL-8, IL-18 and IL1-RA (SI Fig 3). A small number of B-cells positive for IL6, monocytes positive for IL10 and NK cells positive for IFN-g mRNA were present but we did not detect any robust evidence of T-cell activation in our data. Expression of KI-67, a marker of replicating cells, was rarely detected.

Analysing each patient separately, we observed that all possessed lymphocytes assigned to one of the nine B-cell, T-cell or NK cell clusters, although the frequencies varied between patients and for P6 from acute disease to convalescence (Figure 1F and 1G). In contrast, each patient's monocytes were assigned to only one or two clusters specific to each patient/disease state. To explore this in greater detail we repeated dimensionality reduction analyses on just the subset of data representing monocytes. This yielded nine monocytes clusters (numbered mc0 to mc8, Figure 2A) that we aligned to the three canonical monocyte subsets based on CD14 and CD16 expression (SI FIG 4 and 5). Clusters mc0, mc1, mc3, mc4 and mc5 were designated $CD14^{+}$ $CD16^{-}$ classical monocytes (CM), highly phagocytic scavenger cells that comprise 80-90% of monocytes in blood [9]. Cluster mc6 contained $CD14^{int}$ $CD16^{int}$ intermediate monocytes (IM) that play diverse roles in inflammation and angiogenesis [9,10]. Cluster mc2 contained $CD14^{lo}$ $CD16^{hi}$ non-classical monocytes (NCM), also called patrolling monocytes, that actively surveil the vasculature via their expression of CX_3CR1 and exert pro- or anti-inflammatory roles in different contexts [9,11]. CX3CR1 was strongly expressed by cells in mc2 (SI Fig 5).

The IM and NCM subsets are normally rare in blood [9]. The reclustering analysis (Figure 2B) showed the acute sample from KD patient KD2 had high frequencies of IM (8% of total monocytes, cluster mc6) and NCM (38% of total monocytes, cluster mc2). The PIMS-TS patient P6, who like KD2 failed to respond to IVIG, also had an abnormally high frequency of NCM (34% of total monocytes) but lacked IM; upon recovery their monocytes returned to the normal state with only CM detected in their convalescent sample. The acute sample from patient P7, who unlike the other patients responded rapidly to IVIG, lacked IM or NCM. The division of CM into five distinct clusters that varied by disease type and patient severity showed this monocyte subtype is also altered during KD and PIMS-TS. Interestingly, clusterin (CLU), a protein with multiple roles in autoimmunity and inflammation [12], was highly

expressed by CMs during the acute phase of KD and PIMS-TS but not in convalescence Figure 2C, SI Fig 4 and 5). Clusterin has not been reported to be expressed by monocytes [9,13,14].

Our study is the first to reveal that KD and PIMS-TS are both characterised by profound changes in monocyte gene expression and frequencies of key monocyte subpopulations. While supported by a range of known marker genes, our results require confirmation in a larger patient cohort before generalisation. Nevertheless, given the well-known role of monocytes in KD animal models [5,8] and cardiac inflammation and repair [15] the changes we observe are likely to be highly relevant. Measuring monocyte subsets could stratify PIMS-TS and KD patients and predict disease resistance. Agents that modify monocyte function or migration, such as inhibitors of the CX_3CR1/Fractalkine axis [16], could be complementary or alternative therapeutic strategies for KD and PIMS-TS.

References

1. Xu Y *et al*. Characteristics of pediatric SARS-CoV-2 infection and potential evidence for persistent fecal viral shedding. *Nat. Med.* **66,** 502-505 (2020).
2. Feldstein L et al. Multisystem Inflammatory Syndrome in U.S. Children and Adolescents. *N Engl J Med* **383**:334-46 (2020).
3. Whittaker E *et al.* Clinical Characteristics of 58 Children With a Pediatric Inflammatory Multisystem Syndrome Temporally Associated With SARS-CoV-2. JAMA
4. Davies P *et al.* Intensive care admissions of children with paediatric inflammatory multisystem syndrome temporally associated with SARS-CoV-2 (PIMS-TS) in the UK: a multicentre observational study. *Lancet Child Adolesc Healt*h. **20**:30215-7.(2020).
5. Rivas M and Arditi M. Kawasaki disease: pathophysiology and insights from mouse models. *Nat Rev Rheum* **16**:391-405 (2020).
6 McCrindle B *et al.* Diagnosis, Treatment, and Long-Term Management of Kawasaki Disease: A Scientific Statement for Health Professionals From the American Heart Association. *Circulation* **135**:e927–e999 (2017)
7. Katayama K *et al.* CD14+CD16+ monocyte subpopulation in Kawasaki disease. Clin Exp Immunol **121**:566-570 (2000).
8. Stock AT *et al*. The Selective Expansion and Targeted Accumulation of Bone Marrow–Derived Macrophages Drive Cardiac Vasculitis. *J. Immunol.* **202**:3282-3296 (2019).
9. Wong KL *et al*. Gene expression profiling reveals the defining features of the classical, intermediate, and nonclassical human monocyte subsets. *Blood* **118**:e16-e31 (2011).
10. Sampath P et al. Monocyte Subsets: Phenotypes and Function in Tuberculosis Infection. *Front Immunol.* **9**:1726 (2018).

11. Auffray C *et al.* Monitoring of blood vessels and tissues by a population of monocytes with patrolling behavior. *Science* **317**: 666–70 (2007).
12. Falgarone G and Chiocchia G. Clusterin: A Multifacet Protein at the Crossroad of Inflammation and Autoimmunity. Adv. Can. Res. **104**:139-70 (2009).
13. Frankenberger M *et al.* Transcript profiling of CD16-positive monocytes reveals a unique molecular fingerprint. *Eur. J. Immunol.* **42**: 957–974 (2012).
14. Villani A *et al*. Single-cell RNA-seq reveals new types of human blood dendritic cells, monocytes and progenitors. Science. **356**:eaah4573 (2017).
15. Bajpai G et al. The human heart contains distinct macrophage subsets with divergent origins and functions. *Nat. Med*. **24**:1234–1245 (2018).
16. Imai T and Yasuda N Therapeutic intervention of inflammatory/immune diseases by inhibition of the fractalkine (CX3CL1)-CX3CR1 pathway. *Inflamm. Regener*. **36**:9 (2016)

Figure 1

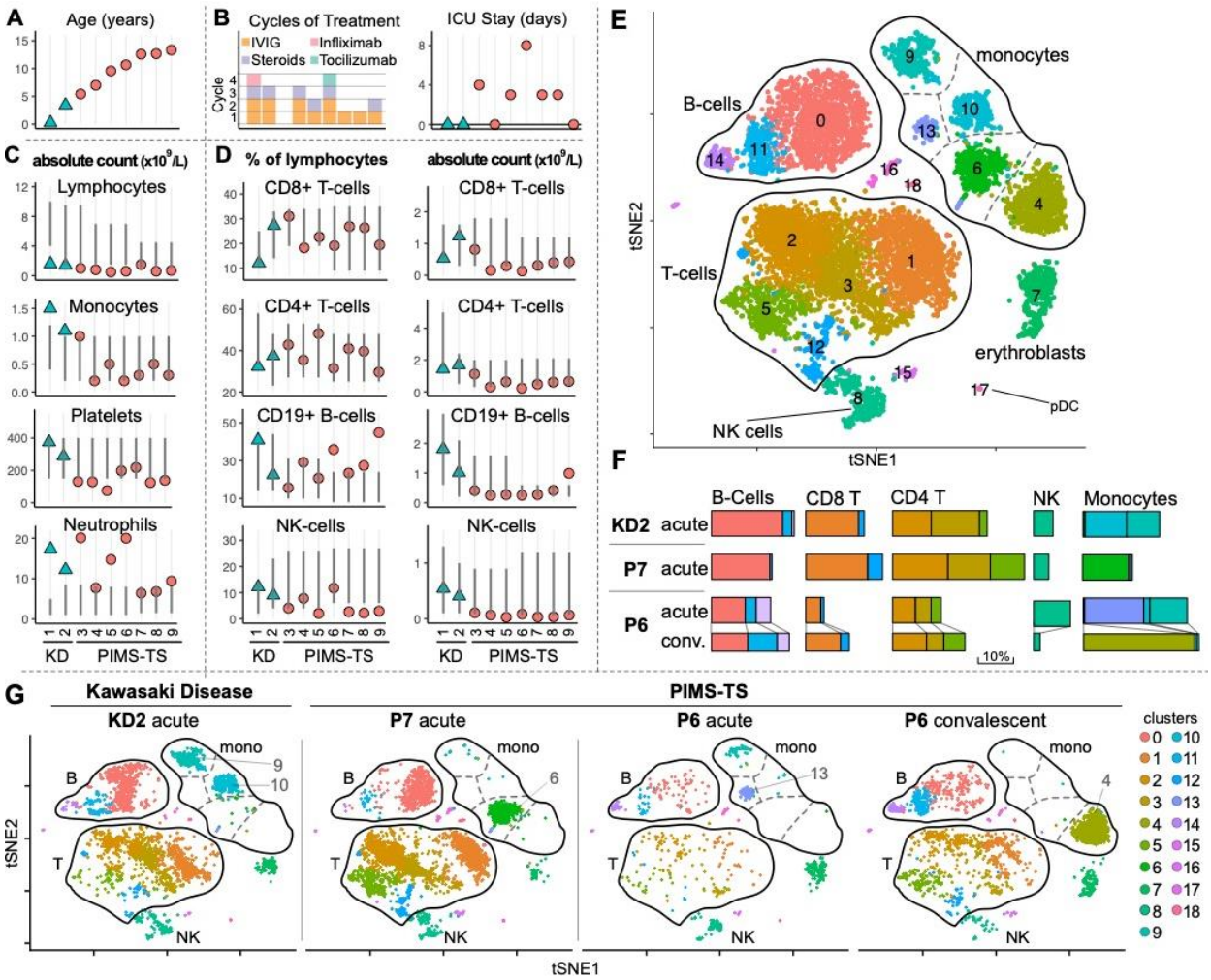

Figure 1. Demographic, clinical and immunological status of nine paediatric patients with Kawasaki disease or PIMS-TS. A. Patient age**. B.** Cycles of treatment and ICU stay. Patient P3 received only aspirin. **C.** Pre-treatment absolute count of different immune cell subsets expressed as 10^9 cells/L. The vertical dark grey bar indicates the normal range for each child based on their age. **D**. Pre-treatment frequency of lymphocyte subsets expressed as the percentage of total lymphocytes (left column) or absolute number of cells x10^9/L (right column). **E**. tSNE representation of major cell types and associated clusters in pre-treatment PBMCs from KD2, P7, P6 and a convalescent sample from P6. **F.** Relative size of PBMC clusters for each patient sample. **G**. tSNE representation of PBMCs from each patient sample.

Figure 2

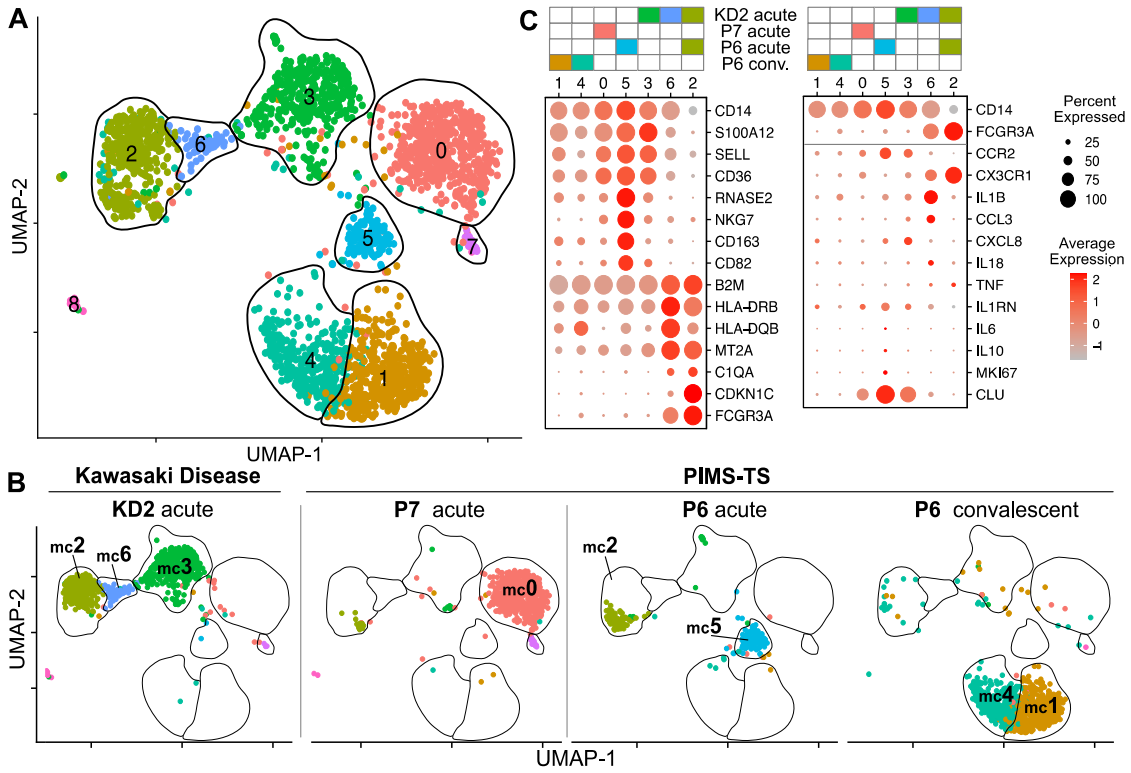

Figure 2. Detailed analysis of monocytes. A. UMAP representation of monocyte clusters in pre-treatment PBMCs from patients KD2, P7, P6 and a convalescent sample from P6 after re-clustering of monocytes alone. **B.** UMAP representation of monocyte clusters from each patient sample. **C.** Expression of select genes in monocyte clusters.

Supplementary information

Methods

Study design, participants and ethical approval

All samples were obtained from children at Birmingham Children's Hospital as part of a Health Research Authority approved study (TrICICL) in accordance with the Declaration of Helsinki. The study was reviewed and approved by South of Birmingham Research Ethics Committee (REC: 17/WM/0453, IRAS: 233593). Written informed consent was obtained from all participants or their legal guardians. Initial presenting features during PICU of five patients with PIMS-TS have been reported in a recent study [4]. Cardiac features in five patients and antibody profiles of four patients have also been presented in our single centre reports [17, 18]. The single cell RNA sequencing analysis reported in the current manuscript has not been published previously.

Blood Samples and PBMC Isolation

Peripheral blood samples from paediatric patients presenting with suspected PIMS-TS were collected in EDTA tubes and stored at room temperature before processing. Peripheral blood mononuclear cells (PBMCs) were isolated using SepMate tubes (Stemcell Technologies) as per the manufacturer's protocol. PBMCs were cryopreserved in medium containing DMSO [19] before transfer to liquid nitrogen for long-term storage. All blood samples used for scRNAseq analysis were processed within 4 hours of phlebotomy.

Data Generation

SARS-CoV-2 antibodies to the viral spike proteins were detected by ELISA as described [18]. Clinical laboratory tests were performed at the Birmingham Children's Hospital's clinical laboratory. Lymphocyte subset enumeration was performed by the University of Birmingham Clinical Immunology Service using BD Trucount™ tubes (CD3,4,8,19,15,56) and analysed using a BD FACS Canto II cytometer. Pediatric reference values were obtained from previously published data [20]. For scRNAseq analysis cryopreserved PBMCs were recovered and feature barcoded using the following DNA-conjugated Totalseq-B antibodies (Biolegend): anti-human TCRg/d, anti-human CD45RO and the TotalSeq-B Human TBNK cocktail designed to react against CD3, CD4, CD8, CD11c, CD16, CD19, CD45 and CD56. Single cell libraries were constructed using 10X Genomics Single Cell 3' Reagents Kits v3 according to manufacturer's instructions and sequenced on an Illumina NextSeq 500 platform.

ScRNAseq Data Pre-processing and Quality Control

Processing of raw reads including 10X barcode-aware demultiplexing from BCL to FASTQ files, transcriptome alignment to human genome assembly GRCh38 and unique molecular

identifier (UMI) counting were performed using the 10X Cell Ranger pipeline version 3.1.0 with GRCh38-version 3.0.0 as the reference. Seurat v3.1.5 [21] was used for sample merging, quality control (QC), clustering and reporting. Both the gene expression (RNA) and antibody-derived tag (ADT) assays were loaded from the CellRanger count platform into a Seurat object for each sample excluding cells with less than 200 genes and features detected in less than 3 cells. The four samples were then merged to create a single aggregated object. QC was conducted on both assays separately. For the RNA assay, to mitigate the influence of sex on clustering and differential expression, the XIST and RSP4Y1 genes were removed. Cells with a number of features between 200 and 600, counts of greater than 1000 and mitochondrial percentage less than 15% were kept for further processing. The gene expression data was normalised using the 'LogNormalize' method with the scale.factor set to the default 10000. 1500 variable features were identified using the 'vst' method of the 'FindVariableFeatures' function. The assay was finally scaled with the number of counts and mitochondrial percentage variables regressed. The ADT assay was first used to identify dead cells or cell doublets by removing double positive instances of lineage markers according to the following criteria: CD14 > 60 & CD19 > 50, CD19 > 40 & CD3 > 40, CD14 > 80 & CD3 > 50 and CD3 < 50 & gamma-delta > 400. The assay was then centred log-ratio (CLR) normalised and scaled with default parameters. The remaining object comprised 10,031 cells with 17,583 features.

PBMC Clustering

Both the RNA and ADT assays were used to compute 50 principal components. These principal components were then used as input into the 'FindNeighbours' function and subsequently the 'FindClusters' function with resolution set to the default value of 1, resulting in 19 clusters. A tSNE reduction was conducted and plotted with 50 dimensions with default perplexity. The clusters were manually annotated from expression of lineage markers both at the transcript (RNA) and protein (ADT) levels. To check our samples for potential T-cell activation we evaluated our data for expression of genes previously identified by scRNAseq analysis as being upregulated upon T-cell stimulation [22].

Monocyte Clustering

To examine the monocyte populations in finer detail, we extracted clusters 4, 6, 9, 10 and 13 from Figure 1E using the 'Subset' function. As monocytes were abundant within each sample, all monocyte clusters were included (2248 monocytes extracted). Both assays were normalized separately again (RNA: 'LogNormalize' & ADT: 'CLR'). The 'vst' method was used to find the 2000 most variable features within the RNA assay and the data was scaled with the variables 'number of counts' and 'percent mitochondria' regressed. The ADT assay was scaled with default parameters. In this instance, 100 principal components were used in the 'RunPCA' function with the top 50 of those components used to find cell neighbours and clusters. The

UMAP reduction was selected here as the clusters visually displayed a better path from classical to intermediate to non-classical monocytes over the tSNE reduction. Nine clusters were originally generated with further assessment resulting in the identification of seven monocyte clusters. CD14 and CD16 markers from the ADT assay were used to classify classical (CD14+), non-classical (CD16+) and intermediate (CD14+CD16+) monocyte populations. Further differential expression analysis of the RNA assay was used to define cellular function within each cluster.

Supplementary References

17. Ramcharan T et al. Paediatric Inflammatory Multisystem Syndrome: Temporally Associated with SARS-CoV-2 (PIMS-TS): Cardiac Features, Management and Short-Term Outcomes at a UK Tertiary Paediatric Hospital *Pediatr Cardiol*. 1-11 (2020).
18. Perez-Toledo M, et al. Serology confirms SARS-CoV-2 infection in PCR-negative children presenting with Paediatric Inflammatory Multi-System Syndrome. Preprint. *medRxiv*. doi.org/10.1101/2020.06.05.20123117 (2020).
19. Kreher, C et al. CD4+ and CD8+ cells in cryopreserved human PBMC maintain full functionality in cytokine ELISPOT assays. *J. Immunol. Methods* **278**, 79–93 (2003).
20. Comans-Bitter W et al. Immunophenotyping of blood lymphocytes in childhood. Reference values for lymphocyte subpopulations. *J Pediatr*. **130**:388-93 (1997).
21. Butler A et al. Integrating single-cell transcriptomic data across different conditions, technologies, and species. *Nat Biotechnol*. **36**:411-420 (2018).
22. Szabo P et al. Single-cell transcriptomics of human T cells reveals tissue and activation signatures in health and disease. *Nature Communications*. 10:4706 (2019).

Reporting Summary

Further information on research design is available in the research reporting summary linked to this article.

Acknowledgements

We thank the children and their families for consenting to join this research study and Birmingham Women's and Children's Hospital Charity for funding the single cell RNA sequencing analysis. ES is supported by a CRUK Birmingham Centre clinical PhD fellowship. BS is funded by a National Institute for Health Research (NIHR) Clinician Scientist fellowship. The views expressed are those of the author(s) and not necessarily those of the NHS, the NIHR or the Department of Health and Social Care. We thank Genomics Birmingham (University of Birmingham) for generating the single cell sequencing data.

We would like to acknowledge staff at the Birmingham Women's and Children's Hospital NHS Foundation trust, including Helen Winmill, Sarah Fox, Carly Tooke, Samantha Owen, Natalie Read, Julie Menzies, Fiona Reynolds, Jim Gray, Mitul Patel, Phillip Hurley, Tristan Ramcharan, Kavitha Masilamani, Habib Ali, Sakeena Samar, Penny Davis, Kathryn Harrison, William Coles, Deevena Chinthala, Heather Duncan, Nick Richens and Sanket Sontakke.

SI TABLE 1

TRICICL-COVID ID	Age range (years)	Sex	Ethnicity	Fever	Rash	Lymph-adenopathy	Conjunctivitis non-exudated	Mucosal changes	Peripheral changes	Cardiac involvement	PCR for SARS-CoV-2	Serology for SARS-CoV-2	Diagnosis
KD1	<5	M	White British	YES	YES	YES	YES	NO	YES	YES	-	-	KD
KD2	<5	M	White British	YES	YES	YES	YES	YES	YES	NO	-	-	KD
P3	<5	M	Black British-African	YES	NO	NO	NO	NO	NO	YES	-	+	PIMS-TS
P4	5-10	M	Asian British-Pakistani	YES	YES	NO	YES	YES	YES	YES	-	+	PIMS-TS
P5	5-10	M	Asian British-Banghladeshi	YES	NO	NO	YES	NO	YES	YES	-	+	PIMS-TS
P6	5-10	F	Black British - African	YES	YES	YES	NO	NO	NO	YES	-	+	PIMS-TS
P7	10-15	F	Mixed white & Black Caribbean	YES	NO	NO	NO	NO	NO	YES	-	+	PIMS-TS
P8	10-15	M	Mixed White & Black Afrocarribean	YES	NO	NO	NO	NO	NO	YES	-	+	PIMS-TS
P9	10-15	F	White/ Romanian	YES	YES	YES	YES	NO	NO	YES	-	+	PIMS-TS

SI Table 1. Demographic and clinical data for the nine patients with Kawasaki Disease or PIMS-TS recruited to the study. KD patients are indicated by grey background. PCR: polymerase chain reaction.

SI TABLE 2

Patient ID	CRP (mg/L)	ESR (mm/h)	Ferritin (µg/L)	Troponin (ng/L)	D-dimer (mg/L)	NT pro-BNP (ng/L)	WCC ($x10^9$/L)	Neutrophils ($x10^9$/L)	Platelets ($x10^9$/L)	Lymphocytes ($x10^9$/L)	Monocytes ($x10^9$/L)
KD1	**127**	N/A	N/A	N/A	N/A	N/A	**28.3**	**17.3**	375	1.6	1.5
KD2	**83**	**32**	271	N/A	**0.89**	N/A	**14.8**	**12.2**	288	**1.4**	1.1
P3	**240**	**75**	312	**671**	**4.85**	**>35000**	**24.8**	**20.1**	132	1.0	1.0
P4	**138**	**62**	**946**	**25**	**3.64**	N/A	9.4	**7.7**	129	**0.8**	0.2
P5	**208**	**33**	**2054**	**2054**	**3.44**	N/A	**16.4**	**14.7**	75	**0.5**	0.5
P6	**342**	**125**	255	**204**	**1.35**	**1929**	**20.6**	**20**	198	**0.6**	0.2
P7	**172**	**52**	368	**1993**	**6.58**	**4233**	8.2	6.4	218	1.5	0.3
P8	**110**	**27**	**510**	**437**	**1.38**	**13465**	8.4	6.8	125	**0.6**	0.5
P9	**131**	**70**	N/A	**N/A**	**1.64**	N/A	10.8	**9.4**	139	**0.7**	0.3

SI Table 2. Clinical laboratory results for the nine patients with Kawasaki Disease (KD) or PIMS-TS recruited to the study. KD patients are indicated by grey background. Abnormal results are shown in bold

SI Figure 1. Gene expression profile of 19 clusters generated from patient PBMC samples.

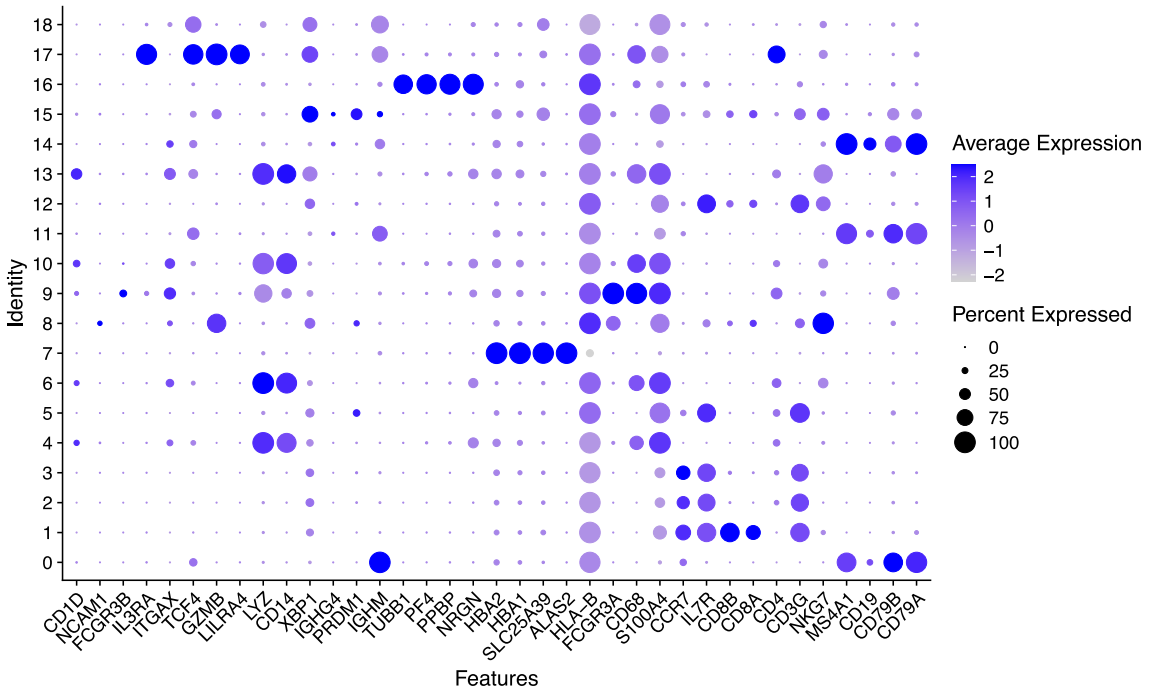

SI Figure 2. Heatmap showing scaled expression of discriminative genes sets for each PBMC cluster. Only the top five discriminative genes per cluster are shown.

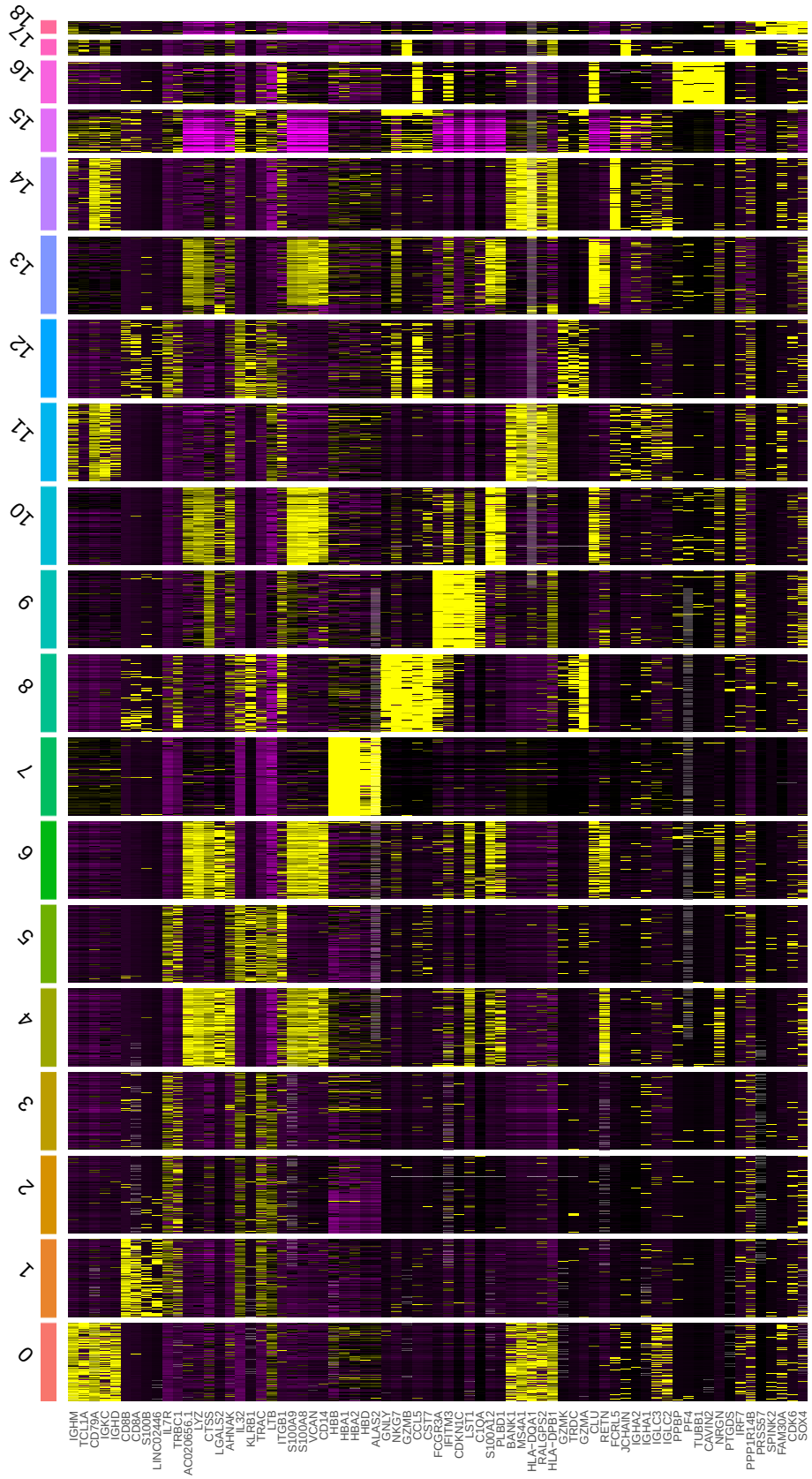

SI Figure 3. RNA expression and protein levels in patient PBMCs.

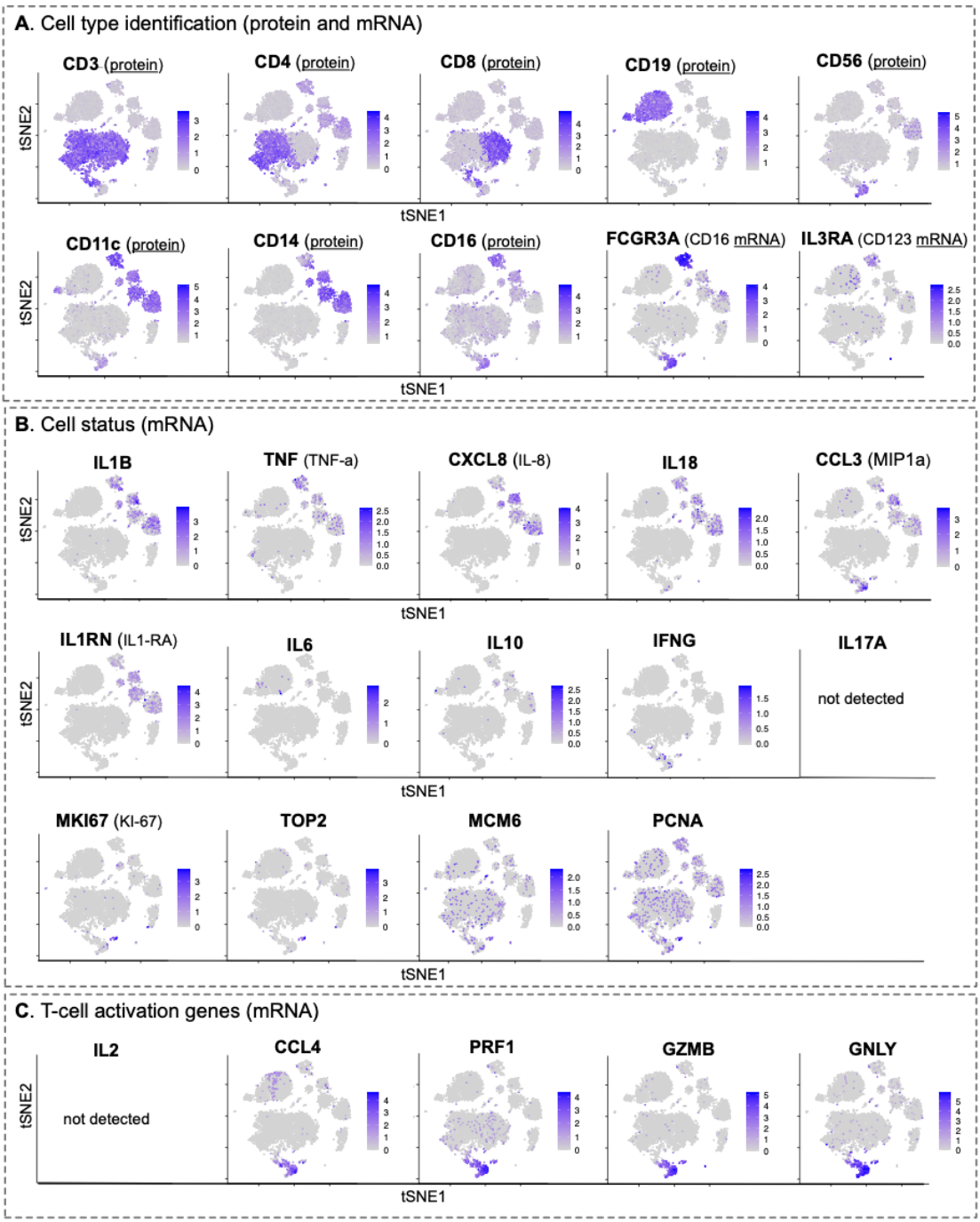

tSNE representation of combined PBMCs from all four patient samples coloured by the level of RNA per cell or level of protein per cell measured using antibody derived tags.

SI Figure 4. Heatmap showing scaled expression of discriminative genes sets for each of the new clusters generated by reclustering of cells from the originally identified monocyte clusters. Only the top five discriminative genes per cluster are shown.

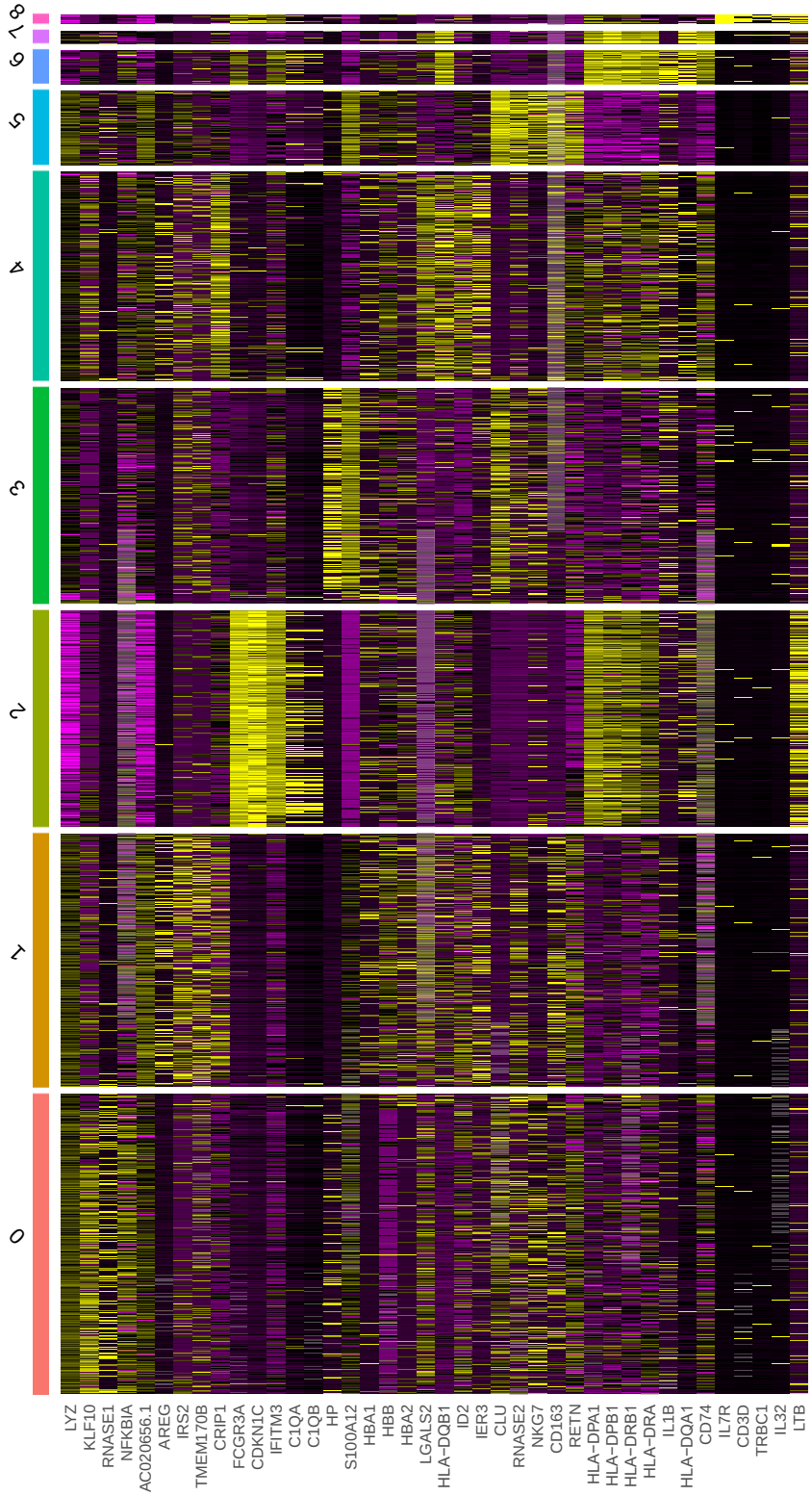

SI Figure 5. RNA expression and protein levels in patient monocytes.

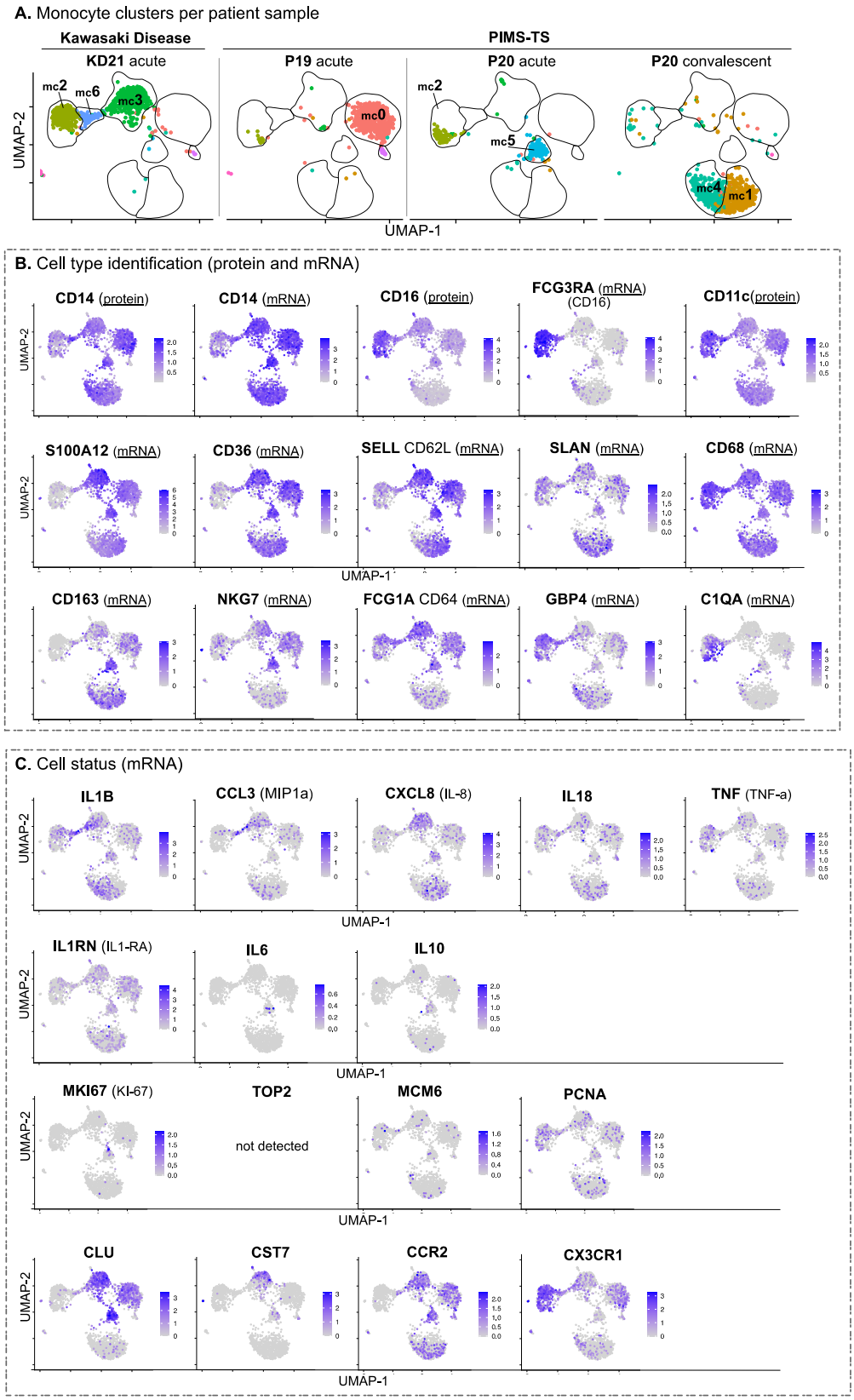

UMAP representation of monocytes from all four patient samples coloured by the level of RNA per cell or level of protein per cell measured using antibody derived tags.